

Multifractal analysis of imprecise data: Badii-Politi and correlation integral approaches

L. V. Meisel and M. A. Johnson

Benet Laboratories, Watervliet Arsenal, Watervliet, New York 12189

(Received 24 February 1994)

Analytic and numerical implementations of the correlation integral and the Badii-Politi multifractal analysis algorithms are described and applied to machine precision and imprecise model multifractal data. The correlation integral technique yields good results for machine precision data and for data with 1% random errors. The *standard* numerical Badii-Politi algorithm did not yield satisfactory results for data with 0.05% or larger random errors. However, the present results suggest that a natural generalization for the Badii-Politi approach along the lines suggested by Kostelich and Swinney [Phys. Scr. **40**, 436 (1989)] can be applied to the analysis of imprecise fractal data.

PACS number(s): 02.70.-c, 05.45.+b

I. INTRODUCTION

A number of algorithms have been devised for the measurement of multifractal dimensions. A selection of such algorithms are described in Refs. [1–11]. The standard algorithms yield the Hentschell-Procaccia [1] fractal dimension $D(q)$, the $f(\alpha)$ spectrum, or other related fractal measures for precise (i.e., machine precision) data.

The consequences of noise on the effectiveness of fractal analysis algorithms has been addressed in Refs. [2] and [3] but not in a systematic way. Reference [2] demonstrated that a box-counting fractal analysis algorithm converged near “true” values for a variety of Koch constructions and mappings based on two- and three-digit “pixel-value” data for $q \geq 0$. Reference [3] demonstrated that a *generalized* Badii-Politi algorithm yielded the correlation dimension $D(2)$ within about 10% for a 2^{18} point subset of points on the Mackey-Glass attractor having 0.5% random perturbations.

This paper describes the results of applying two mul-

tifractal analysis techniques to imprecise fractal data. The correlation integral method [4–6] and a *generalized* Badii-Politi procedure are used to determine the consequences of small errors in the coordinates of points comprising subsets of standard fractal constructions [12,13] in R^2 . The correlation integral algorithm is of the customary form, except that automated procedures for selecting the scaling range are employed. The *generalized* Badii-Politi algorithm is essentially equivalent to that applied by Kostelich and Swinney [3] in their determinations of $D(2)$; it reduces to the *standard* Badii-Politi algorithm [7] as a special case.

II. BACKGROUND

A. The correlation integral algorithm

1. Analytic correlation integral algorithm

The correlation integral is defined as

$$C(q, E) \equiv \left\{ \int_{\Omega} d\vec{x} \rho(\vec{x}) \left[\int_{|\vec{y}| \leq E} d\vec{y} \rho(\vec{x} + \vec{y}) \right]^{q-1} \right\}^{1/(q-1)} \quad (1a)$$

$$= \left\{ \int_{\Omega} d\vec{x} \rho(\vec{x}) \left[\int_{\Omega} d\vec{y} \rho(\vec{y}) H(E - |\vec{x} - \vec{y}|) \right]^{q-1} \right\}^{1/(q-1)}, \quad (1b)$$

where Ω is the volume containing the fractal set, $\rho(\vec{x})$ is the density of the set at \vec{x} , and $H(x)$ is the Heaviside function.

For a discrete fractal set, the correlation integral Eq. (1b) takes the form

$$C(q, E) = \lim_{N \rightarrow \infty} \left\{ \frac{1}{N} \sum_k \left[\frac{1}{N} \sum_j H(E - |\vec{x}_k - \vec{x}_j|) \right]^{q-1} \right\}^{1/(q-1)}, \quad (1c)$$

where \vec{x}_j and \vec{x}_k run over N -element fractal subsets. It is shown that the Hentschell and Procaccia fractal dimension is then given by

$$D(q) = \lim_{E \rightarrow 0^+} \frac{\ln(C(q, E))}{\ln(E)}. \quad (2)$$

2. The numerical correlation integral method

The numerical correlation integral method is based on

$$C(q, E) \approx \left\{ \frac{1}{N_{\text{ref}}} \sum_k^{N_{\text{ref}}} \left[\frac{1}{N} \sum_j^N H(E - |\bar{x}_k - \bar{x}_j|) \right]^{q-1} \right\}^{1/(q-1)} \sim E^{D(q)}, \quad (3)$$

where j runs over the N -element fractal subset and k runs over an N_{ref} element randomly selected subset of the fractal set in question. Equation (3) represents approximations to Eqs. (1c) and (2).

The correlation integrals $C(q, E)$ are generally evaluated for a set of q values of interest and a logarithmically spaced set of E values chosen to cover the range of scales in the fractal subset. The smallest E is chosen to be of the order of the largest nearest neighbor spacings in the data set. The largest E is chosen to be approximately a diameter of the data set. The fractal dimension $D(q)$ is then obtained by least squares fitting to the linear portion of $\ln[C(q, E)]$ vs $\ln[E]$.

An automated procedure was developed for the selection of ranges of $\ln[E]$ and the determination of $D(q)$ for fitting to Eq. (3). The limits on $\ln[E]$ and the values of $D(q)$ are obtained by averaging the lowest rms error fits over ranges of consecutive $\ln[E]$. The minimum number of $\ln[E]$ values is made small enough to fit into the linear range, yet large enough to avoid small straight runs of points. This procedure is described in more detail in the Appendix.

B. The Badii-Politi algorithm

1. Analytic Badii-Politi algorithm

The Badii-Politi algorithm is designed for application to discrete fractal data. The technique focuses on the probability distribution $P(\delta, n)$ of the nearest neighbor distances δ among n -point subsets. The moments of the distribution of nearest neighbor distances are shown to vary asymptotically as $n^{-\gamma/D(\gamma)}$, where $D(\gamma)$ is a ‘‘dimension’’ which can be related simply to $D(q)$. Explicitly,

$$\langle \delta^\gamma \rangle \equiv M(\gamma, n) \equiv \int_0^\infty \delta^\gamma P(\delta, n) d\delta \sim n^{-\gamma/D(\gamma)} \quad (4)$$

The dimension $D(\gamma)$, which Ref. [3] refers to as ‘‘the dimension function,’’ is given by

$$D(\gamma) = \lim_{n \rightarrow \infty} \frac{-\gamma \ln(n)}{\ln(M(\gamma, n))}. \quad (5)$$

The Badii-Politi approach is closely related to that espoused by Halsey *et al.* [14]. For example, Ref. [7] demonstrates how the analytic Badii-Politi algorithm can be applied to determine the multifractal measures of Koch constructions by analysis of their generators along the lines described in Halsey *et al.* [14]. One can translate the Badii-Politi expressions into ‘‘standard notation,’’ i.e., the notation of Renyi [15] or Halsey *et al.* [14], by the replacements

$$\gamma \rightarrow -\tau \quad \text{and} \quad D(\gamma) \rightarrow D(q)$$

which imply that

$$-\gamma/D(\gamma) \rightarrow q - 1$$

since $\tau(q) = (q - 1)D(q)$. Thus Eq. (4) becomes

$$\langle \delta^{-\tau} \rangle \equiv M(\tau, n) \equiv \int_0^\infty \delta^{-\tau} P(\delta, n) d\delta \sim n^{q-1}. \quad (4')$$

2. The standard numerical Badii-Politi algorithm

Badii and Politi approximate the integral expression for $M(\gamma, n)$, etc. as

$$M(\gamma, n) \approx \frac{1}{n} \sum_{j=1}^n \delta_j^\gamma(n) \sim n^{-\gamma/D(\gamma)} \quad (6)$$

define the ‘‘ γ volume’’ $\tilde{L}(\gamma, n)$ as

$$\tilde{L}(\gamma, n) \equiv nM(\gamma, n) \approx \sum_{j=1}^n \delta_j^\gamma(n) \sim n^{1-\gamma/D(\gamma)} = n^q, \quad (7)$$

where δ is taken as the third nearest neighbor distance, and compute $D(\gamma)$ from the scaling of $\tilde{L}(\gamma, n)$, with the number n of randomly chosen points in the subsets in which the third nearest neighbor distances are found. For each n , a subset of n points is taken as a ‘‘reference set.’’ [For example, the average, defining $\tilde{L}(\gamma, 8)$ or $M(\gamma, 8)$, is based on eight randomly selected points.]

3. A generalized numerical Badii-Politi algorithm

A generalized form of the numerical Badii-Politi algorithm, similar to that employed by Kostelich and Swinney [7] to determine the correlation dimension, is used. It is based on Eq. (4') rather than Eq. (5). The principal differences from the numerical algorithm of Ref. [3] are the following.

(1) A fixed, relatively large reference set is employed for all values of n . The use of a larger reference set, especially at small n , substantially reduces the variability of $M(\tau, n)$ under different random point selections. A substantially larger reference set (which essentially eliminated the dependence of results on the random point selection procedure) than that employed in Ref. [3] was employed in the present studies.

(2) The neighbor number η is allowed to vary. That is, the scaling of nearest neighbor number distances for a variety of neighbor numbers (η) are considered. *Standard* numerical Badii-Politi algorithm results are obtained for the special case of third nearest neighbor ($\eta=3$) distances.

Thus, translating into the notation of Halsey *et al.* [14], the generalized Badii-Politi algorithm takes the form

$$M(\tau, n) \approx \frac{1}{N_{\text{ref}}} \sum_{j=1}^{N_{\text{ref}}} \delta_j^{-\tau}(n) \sim n^{q-1}, \quad (8)$$

where δ can be the distance to an arbitrary η , and N_{ref} is independent of n .

III. RESULTS AND DISCUSSION

The Badii-Politi and correlation integral numerical algorithms were tested on a variety of constructions in R^2 for which analytic $D(q)$ values are known. The algorithms were applied to Euclidean point sets, Koch asymmetric snowflake fractals based on a four element generator having two 0.4 and two 0.2 length elements, symmetric triadic snowflakes [12], split snowflake halls [12], and the 13 element generator Koch construction [12]. The attractor of the sixfold ($D6$) symmetric chaotic mapping described by Field and Golubitsky [13] was also studied. Imprecise data were produced by perturbing the x and y coordinates of the fractal points by “random” values.

The results of extensive analysis of 1.97×10^5 point subsets of the asymmetric snowflake fractal are presented. Similar results were obtained for all the fractal cases studied. Reference [16] demonstrates that 10^5 point subsets of the asymmetric snowflake are large enough to ensure 1% convergence of the correlation integral method over the range $-25 \leq q \leq 25$. Although we are aware of no systematic study of convergence for the Badii-Politi procedure, the analysis of Broggi and co-workers [17] suggests that 1.97×10^5 points are sufficient for $D(0) \approx 2$. The results of Kostelich and Swinney [3] suggest that substantially smaller point sets may be sufficient. Also, Ref. [2] established that 10^4 points are sufficient for 1% convergence of a box-counting algorithm for the asymmetric snowflake in the range $0 \leq q \leq 25$.

Figure 1 shows 1.23×10^4 point subsets of the asymmetric snowflake fractal with 0.0, 0.5, 1.0, and 2.5% random errors on each axis. Perturbations of the order of 0.5% are easily perceived.

Figure 2 shows $\ln[C(-12, E)]$ vs $\ln[E]$ for 1.97×10^5 point subsets of the asymmetric snowflake fractal with 0.0, 0.05, and 0.5% random errors. The correlation integral values were computed with $N_{\text{ref}} = N/5$ for 40 log spaced E values, and were indistinguishable from those computed for $N_{\text{ref}} = N$.

The vertical lines show the averaged upper and lower limits of the range of $\ln[E]$ that were selected by the automated procedure using the 20 lowest rms error fits with runs of a minimum of 20 consecutive $\ln[E]$ values. It is apparent that they are near “breaks” in the curves, and closely approximate the linear boundaries. Essentially the same results were obtained using the ten lowest rms error fits and a minimum of ten consecutive $\ln[E]$ values.

These results suggest that the 0.5% random errors introduced into the Mackey-Glass attractor by Kostelich and Swinney [3] (which are of the order of the uncertainties in their experimental Couette-Taylor data) were not sufficiently large to effect the correlation integral analysis for the range of hypersphere radii (viz. $-6 < \log_2(\epsilon) < -1$) employed in their analysis. One

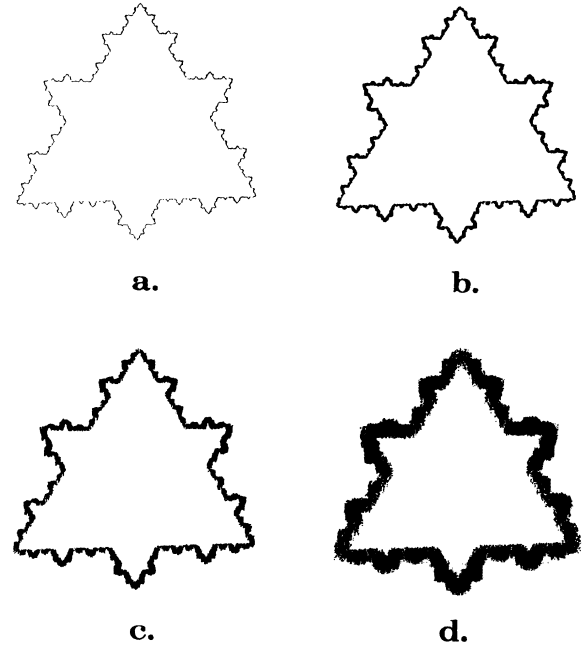


FIG. 1. 1.23×10^4 point subsets of the asymmetric snowflake fractal with (a) 0.0, (b) 0.5, (c) 1.0, and (d) 2.5% random errors.

would expect to find “breaks” and tangible effects in the correlation integral analysis for $\log_2(\epsilon) \approx \log_2(0.005) \approx -7.6$, which is substantially to the left of the range of $\log_2(\epsilon)$ employed in their analyses.

Note that the linear portion for the 0.5% data in Fig. 2 comprises about one order of magnitude variation in the correlation integral hypersphere radii, and that this restricted range of $\ln[E]$ is still sufficiently large to yield

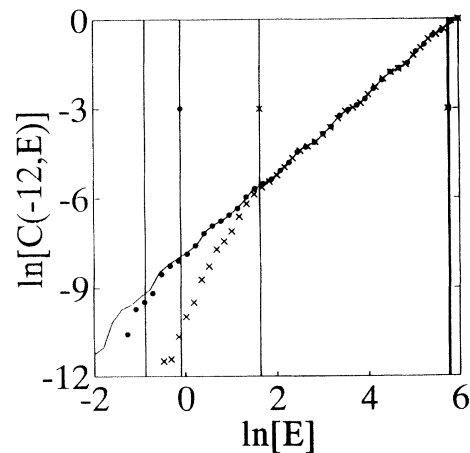


FIG. 2. $\ln[C(-12, E)]$ vs $\ln[E]$ for 1.97×10^5 point subsets of the asymmetric snowflake fractal with 0.0 (solid line), 0.05 (filled circles), and 0.5% (\times 's) random errors. The vertical lines are the averaged upper and averaged lower limits automatically selected for the range of $\ln[E]$. The limits for the precise data are unmarked, for 0.05% data are marked with a filled circle, and those for 0.5% data are marked with an \times .

1% agreement between the measured and analytic $D(q)$ values [see Fig. 4(b)].

Figure 3 shows $\ln[M(n, \gamma)]$ vs $\ln[n]$ based on the *standard* Badii-Politi numerical algorithm ($\eta=3$) for $-\gamma/D(\gamma)+1=\tau/D(q)+1=q$, for $q \approx -12, 0$, and 12 for 1.97×10^5 point subsets of the asymmetric snowflake fractal with 0.0, 0.05, and 0.5% random errors. The Badii-Politi $M(n, \gamma)$ values were computed for 20 log spaced n values. The $M(n, \gamma)$ values shown were computed with $N_{\text{ref}}=N/5$. Unlike the data in Fig. 2 (where breaks are apparent), there is no indication that the curves obtained from the imprecise fractal data should be treated differently or that analysis of the imprecise data will yield unreliable results.

Figure 4 presents $D(q)$ vs q curves determined by means of the *standard* numerical Badii-Politi algorithm for 1.97×10^5 point subsets of the asymmetric snowflake fractal with 0.0, 0.05, and 0.5% random errors. The solid line is the analytic $D(q)$ vs q result. The dense set of points near $q=0$ plus the point near $q=5$ span the range of the Table in Ref. [7]. The *standard* Badii-Politi technique returns $D(-1 < q < 5)$ within 1% of the analytic values and $D(-5 < q < 25)$ values within 5% for precise fractal data. However, the results are poor for q outside this range, and small random errors of the order 0.05% push the results up near $D(q)=2.0$ (the random point set value).

Figure 5 shows $D(q)$ vs q curves determined by the correlation integral algorithm for the same data and on the same scale as Fig. 4. The solid line is the analytic $D(q)$ vs q result. The correlation integral results are within 1% of the analytic values of $D(q)$ except for a small range near $q=-5$.

Figure 6 shows correlation integral algorithm results for $D(q)$ vs q for 1.97×10^5 point subsets of the asymmetric snowflake fractal with 0.0, 0.5, 1.0, and 2.5% random errors. The solid line is the analytic $D(q)$ vs q result. Although satisfactory results were obtained for 1% fractal data, substantial errors in the measured $D(q)$ ap-

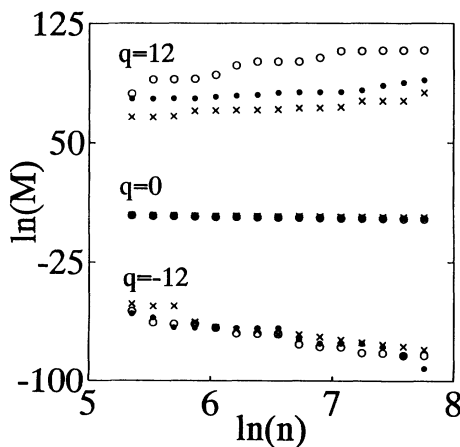


FIG. 3. $\ln[M(n, \gamma)]$ vs $\ln[n]$ for $q \approx -12, 0$, and 12 for 1.97×10^5 point subsets of the asymmetric snowflake fractal with 0.0 (open circles), 0.05 (filled circles), and 0.5% (\times 's) random errors.

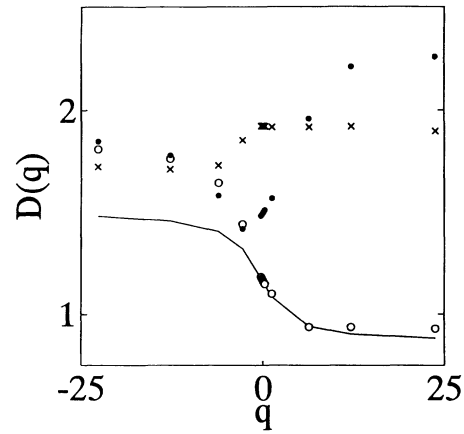


FIG. 4. $D(q)$ vs q results using the *standard* numerical Badii-Politi algorithm for 1.97×10^5 point subsets of the asymmetric snowflake fractal with 0.0 (open circles), 0.05 (filled circles), and 0.5% (\times 's) random errors. The solid line is the analytic solution.

pear for 2.5% random errors.

Figure 7 presents $D(q)$ vs q results determined by the *generalized* Badii-Politi numerical algorithm using 0.05% data for 1.97×10^5 point subsets of the asymmetric snowflake fractal. The numbers to the left of the curves designate the neighbor number used in the *generalized* Badii-Politi numerical algorithm. $D(q \geq 0)$ were within 2% of analytic values for $81 \leq \eta \leq 130$, and $D(q < 0)$ were within 5% for $81 \leq \eta \leq 180$ for the asymmetric snowflake. Similar effects were observed for the other 0.05% constructions studied here.

Since the averaged 81st nearest neighbor distances are larger than the 0.05% uncertainty in the fractal data set, and the averaged third nearest neighbor distances are of the order of the 0.05% uncertainty in the fractal data set,

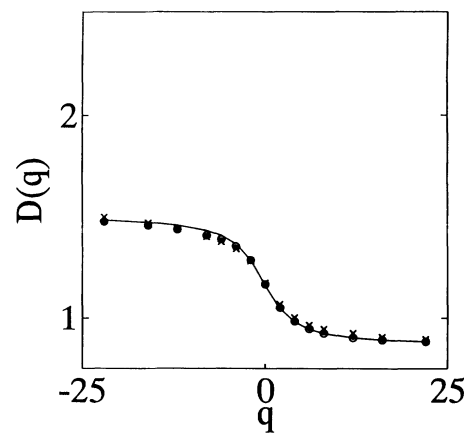


FIG. 5. $D(q)$ vs q results using the numerical correlation integral algorithm for 1.97×10^5 point subsets of the asymmetric snowflake fractal with 0.0 (open circles), 0.05 (filled circles), and 0.5% (\times 's) random errors. The solid line is the analytic solution.

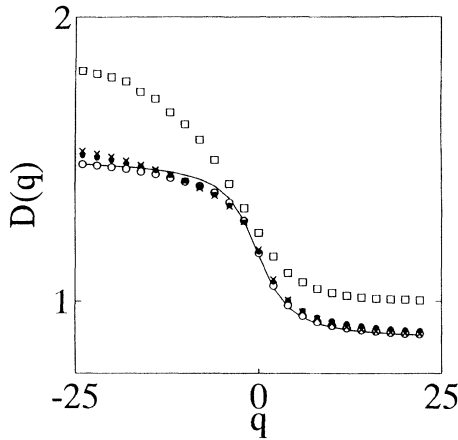


FIG. 6. $D(q)$ vs q results using the numerical correlation integral algorithm for 1.97×10^5 point subsets of the asymmetric snowflake fractal with 0.0 (open circles), 0.5 (filled circles), 1.0 (\times 's), and 2.5% (open square) random errors. The solid line is the analytic solution.

it is not surprising that the scaling for $\eta \geq 81$ gives a better representation than that of the third neighbors for 0.05% data. (This effect of increasing η is the motivating idea for the *generalized* Badii-Politi algorithm.)

Equivalent *generalized* Badii-Politi results were reported in Ref. [3] for the correlation dimension $D(2)$ measured in Couette-Taylor flows for a range of Reynolds numbers, and in numerical realizations of the Mackey-Glass attractor. [The monotonic decreasing $D(q \geq 0)$ with increasing η evident in Fig. 7, and for the correlation dimension in Ref. [3] is not the general case in the present study or in the results reported in Ref. [17].]

The $\ln[M(n, \gamma)]$ vs $\ln[n]$ curves do not reveal the range of η which yield "best results." For example, $\ln[M(n, \gamma)]$ vs $\ln[n]$ curves that fit Eq. (8) with small rms

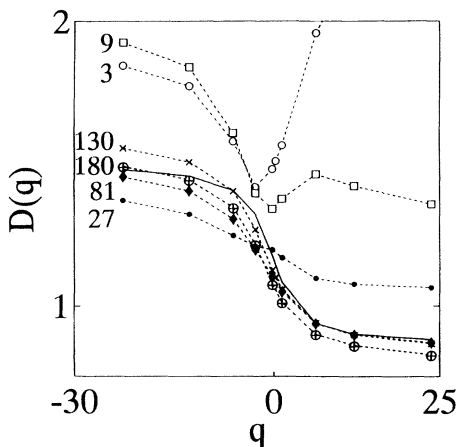


FIG. 7. $D(q)$ vs q results using the *generalized* numerical Badii-Politi algorithm for 1.97×10^5 point subsets of the asymmetric snowflake fractal with 0.05% random errors. The neighbor number appears to the left of the corresponding result. The solid line is the analytic solution.

errors, often yield poor $D(q)$. Kostelich and Swinney [3] made essentially the same comment with respect to their *generalized* Badii-Politi algorithm determinations of the correlation dimension.

IV. CONCLUSIONS

The correlation integral method yielded better values of $D(q)$ than the *generalized* Badii-Politi technique in all cases of noisy fractal data studied here. The numerical correlation integral method calculations reported here yielded $D(q)$ values within 1% of analytic values for 0.5% (and machine precision) representations of the multifractal point sets studied except for a small range near $q = -5$. [$D(q)$ values having errors of the order of one percent are also obtained for one percent representations.]

The correlation integral method succeeded in extracting $D(q)$ from the noisy fractal data because longer range fractal scaling is not substantially effected by the imprecision of the data. Restricting the fitting to the linear portion of the $\ln[C(q, E)]$ vs $\ln[E]$ curves excludes the small "hypersphere" correlation integrals from the analysis. The range of $\ln[E]$ to exclude in the determination of $D(q)$ is apparent in the $\ln[C(q, E)]$ vs $\ln[E]$ plots and does not require *a priori* knowledge of the uncertainties in the data. The correlation integral method breaks down when the uncertainty in the location of the points becomes so large that the linear range in the $\ln[C(q, E)]$ vs $\ln[E]$ plots is inadequate.

The *standard* numerical Badii-Politi algorithm gave $D(-1 < q < 5)$ values within 1% of the analytic values and $D(-5 < q < 25)$ values within 5% for machine precision data. On the other hand, the *standard* Badii-Politi algorithm failed at all q when errors on the order of 0.05% were introduced.

The *generalized* numerical Badii-Politi algorithm is less sensitive to noise than the *standard* approach. However, we were unable to determine "optimal" parameters by examining $\ln[M(\tau, n)]$ vs $\ln[n]$ curves. Kostelich and Swinney [3] and Broggi and co-workers [17] discussed the selection of parameters in the Badii-Politi procedure, but were also unable to establish criteria for optimal parameter selection. Our results and those in Ref. [3] imply that the nearest neighbor number used in the *generalized* Badii-Politi algorithm must be sufficiently large that the weighted average distances exceed the uncertainty in the positions of the fractal set.

$D(q < 0)$ for $81 \leq \eta \leq 180$ were within 5% for the asymmetric snowflake and within 7% for the other constructions. $D(q \geq 0)$ for $81 \leq \eta \leq 130$ were within 2% for the asymmetric snowflake and were generally about 5% low for the other constructions studied here. This observation is comparable with the results reported in Kostelich and Swinney [3], where 300th neighbor Badii-Politi results for $D(2)$ for the Mackey-Glass attractor is about 10% lower than the analytic value (i.e., 6.8).

We believe that both the *generalized* Badii-Politi and correlation integral algorithms can be successfully applied to imprecise data in high D cases. However, problems such as restricted linear scaling ranges and lack of

convergence remain unresolved.

A final point in regard to analysis of imprecise fractal data is in order. If the fractal point set in question is the result of invariant embedding of a chaotic time series, then preprocessing of the data along the lines described by Kostelich and co-workers [18] may effect significant noise reduction.

APPENDIX

The automated procedure for correlation integral computation of $D(q)$ is the following:

- (1) Specify two numbers.
- (a) A minimum number of consecutive logarithmically spaced $\ln[E]$ values to be contained in an allowable

“linear range.” This number should be large enough to avoid local straight runs of points and small enough to fit into the “linear range.”

(b) The number of ranges to include in determining $D(q)$. Since the $\ln[C(q, E)]$ vs $\ln[E]$ points tend to oscillate around a straight line, “best” results are obtained by averaging over sets of consecutive $\ln[E]$ values that terminate at high and low $\ln[C(q, E)]$ values.

(2) Make least square fits to Eq. (3) for all ranges of $\ln[E]$ consistent with (1a).

(3) Sort the results on rms errors in slope.

(4) Average values over the lowest rms error cases up to the number specified in (1b) and return the averaged smallest $\ln[E]$ value, the averaged largest $\ln[E]$ value, and the averaged $D(q)$ value.

-
- [1] H. G. E. Hentschel and I. Procaccia, *Physica D* **8**, 435 (1983).
 - [2] L. V. Meisel, M. Johnson, and P. J. Cote, *Phys. Rev. A* **45**, 6989 (1992).
 - [3] E. J. Kostelich and H. L. Swinney, *Phys. Scr.* **40**, 436 (1989).
 - [4] K. Pawelzik and H. G. Schuster, *Phys. Rev. A* **35**, 481 (1987).
 - [5] H. Atmanspacher, H. Scheingraber, and G. Wiedenmann, *Phys. Rev. A* **40**, 3954 (1989).
 - [6] G. Paladin and A. Vulpiano, *Lett. Nuovo Cimento* **41**, 82 (1984).
 - [7] Remo Badii and Antonio Politi, *J. Stat. Phys.* **40**, 725 (1985).
 - [8] A. Block, W. von Bloh, and H. J. Schellnhuber, *Phys. Rev. A* **42**, 1869 (1990).
 - [9] X. J. Hou, R. G. Gilmore, G. B. Mindlin, and H. G. Solari, *Phys. Lett. A* **151**, 43 (1990).
 - [10] Mogens H. Jensen, Leo P. Kadanoff, Albert Libchaber, Itamar Procaccia, and Joel Stavans, *Phys. Rev. Lett.* **55**, 2798 (1985).
 - [11] L. S. Liebovitch and T. Toth, *Phys. Lett. A* **141**, 386 (1989).
 - [12] See, for example, B. B. Mandelbrot, *Fractal Geometry of Nature* (Freeman, New York, 1983). (13-element construction: p. 69. Split snowflake halls: p. 146.)
 - [13] M. Field and M. Golubitsky, *Comput. Phys.* **4**, 470 (1990).
 - [14] Thomas C. Halsey, Mogens H. Jensen, Leo P. Kadanoff, Itamar Procaccia, and Boris I. Shraiman *Phys. Rev. A* **33**, 1141 (1986).
 - [15] A. Renyi, *Probability Theory* (North-Holland, Amsterdam, 1970).
 - [16] L. V. Meisel and M. A. Johnson (unpublished).
 - [17] G. Broggi, *J. Opt. Soc. Am B* **5**, 1020 (1988); M. Ravani, B. Derighetti, G. Broggi, and E. Brun, *ibid.* **5**, 1029 (1988).
 - [18] E. J. Kostelich and J. A. Yorke, *Physica D* **41**, 183 (1990); E. J. Kostelich, *ibid.* **58**, 138 (1992); E. J. Kostelich and T. Schreiber, *Phys. Rev. E* **48**, 1752 (1993).

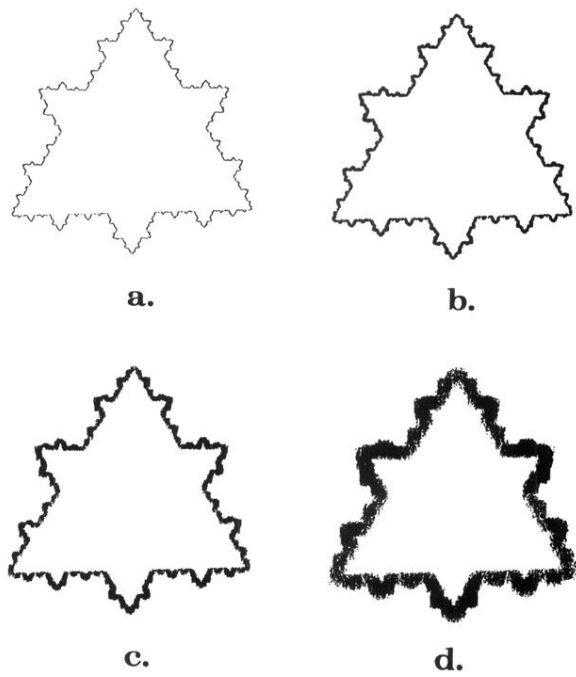


FIG. 1. 1.23×10^4 point subsets of the asymmetric snowflake fractal with (a) 0.0, (b) 0.5, (c) 1.0, and (d) 2.5% random errors.